Theor Chem Acc (2007) 118:173–183
DOI 10.1007/s00214-007-0259-9

REGULAR ARTICLE

About the intrinsic photochemical properties of the 11-cis retinal chromophore: computational clues for a trap state and a lever effect in Rhodopsin catalysis

Alessandro Cembran · Remedios González-Luque · Luis Serrano-Andrés · Manuela Merchán · Marco Garavelli

Received: 27 November 2006 / Accepted: 17 January 2007 / Published online: 22 February 2007

Abstract CASPT2//CASSCF/6-31G* computations are used on the singlet S_1 and S_2 states to map the photoisomerization process of the 11-cis retinal protonated Schiff base in vacuo and to characterize its optical properties. It is shown that the spectroscopic observations recorded in Rhodopsin are reproduced quite well, calling for a substantially neutral effect of the protein. Furthermore, a rationale is proposed for the unreactive population recently observed in Rhodopsin, which is here addressed to the accessible S_2 state, behaving as a trap. The experimental transient absorption and (absorption-wavelength dependent) emission are discussed and interpreted under the light of this novel model. Finally, a planarization of the β-ionone ring is observed on S_1, which may cause a steric lever effect into the protein pocket, thus assisting photoisomerization catalysis. The reported results constitute a solid reference for further studies aimed to rationalize the effect of the environment on the photochemical reactivity of retinal chromophores.

Keywords Ab initio calculations · Reaction mechanisms · Photoisomerization · Retinal · Conical intersections

1 Introduction

The protonated Schiff base (PSB) of retinal is the chromophore of rhodopsin proteins [1–6]. These include the retina visual pigment of animals rhodopsin (Rh), the proton and chloride pumping pigments of *Halobacterium halobium* bacteriorhodpsin (bR) and halorhodopsin (hR) respectively, and other bacterial pigments such as sensory rhodopsins (sR). The biological activity of rhodopsins is triggered by the ultrafast (200 fs in Rh, see Eq. 1) light-induced *cis-trans* isomerization of the corresponding retinal chromophores that, in turn, induces a conformational change in the protein [1,5]. This photochemical step is usually referred to as the primary event of the protein photocycle.

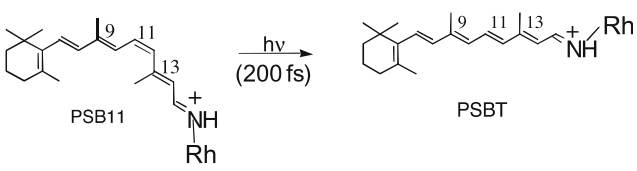

Equation 1

Results of ab initio CASPT2//CASSCF minimum energy path (MEP) mapping for the photoisomerization

Electronic supplementary material The online version of this article (doi:10.1007/s00214-007-0259-9) contains supplementary material, which is available to authorized users.

Contribution to the Fernando Bernardi Memorial Issue.

A. Cembran · M. Garavelli (✉)
Dipartimento di Chimica "G. Ciamician",
Università di Bologna, via Selmi 2, Bologna, 40126 Italy
e-mail: marco.garavelli@unibo.it

Present Address:
A. Cembran
Department of Chemistry and Supercomputing Institute,
University of Minnesota, Minneapolis, MN 55455-0431, USA

R. González-Luque · L. Serrano-Andrés · M. Merchán
Departamento de Química Física,
Instituto de Ciencia Molecular, Universitat de València,
Dr. Moliner 50, Burjassot 46100 Valencia, Spain

in vacuo of reduced models of the retinal chromophore have been recently reported [7–9] These include, among the others, the 11-*cis* (PSB11) retinal chromophore model 4-*cis*-γ-methylnona-2,4,6,8-tetraeniminium cation **1** [8,10,11] and the minimal PSB models all-*trans*-hepta-2,4,6-trieniminium **2** [7] and 2-*cis*-penta-2,4-dieniminium **3** [12] cations (see Scheme 1). Despite the different length of the conjugated chains, it has been shown that the photochemical behavior of these systems is similar, the reaction mechanism being characterized by a two-mode—first stretching then torsion—photoisomerization path on the spectroscopic (charge transfer) state S_1, which is essentially barrierless and drives the system into a central double bond twisted S_1/S_0 conical intersection (CI) funnel. It is worth noting, however, that an extended energy plateau emerges in the initial part of the reaction pathway (see Scheme 1) as the length of the model to approach the real (retinal) chromophore is increased. Eventually, this leads to a very shallow planar minimum (see model **1**). This fact contrasts with the subpicosecond photoisomerization observed in Rhodopsin (Rh), [7,9] arising questions on the origin of the protein catalytic effect that makes this process as one of the fastest photochemical reactions observed so far in nature. Anyway, all these systems represent reduced models of the chromophore and may lack important mechanistic details and quantitative effects. For instance, the lack of the β-ionone ring may be a significant source of errors since it affects the energies (due to the additional conjugated double bond of the ring) [13] and its interaction with the surrounding environment may be not negligible.

Herein, we report for the first time the state-of-the-art fully unconstrained CASPT2//CASSCF/6-31G* MEP computations for the photo-reaction paths of the *real* (i.e. unreduced) 11-*cis* retinal Protonated Schiff Base (PSB11) in vacuo. In particular, we provide information on (1) the structure of the singlet manifold along the fully optimized paths on S_1 and S_2; (2) the spectroscopic properties (i.e. vertical absorption and transient absorption/emission features) and (3) the structure of the photoisomerization reaction coordinate. While we do not want to reject or question out other effects which have been previously presented, discussed and proved, here we will present theoretical innovative arguments that suggest novel scenarios on the mechanism of both the catalysis and unreactive population trapping recently observed in Rh.[14] A thoughtfully discussion of all the most recent experimental findings compared to the new computational results is presented, which supports this new view.

2 Computational details

A complete active space of 12 π-electrons in 12 π-orbitals (12e/12o) and the 6–31G* basis set have been employed to describe the CASSCF wavefunction. Single-root computations have been performed for the first 10 au of the S_1 MEP, then the wavefunction has been described equally weighting the S_0 and S_1 states in a state-averaged procedure to avoid root-flipping problems.

This MEP has been computed from the FC point on the S_1 state to the CI following the prescriptions described in [15,16] and the procedure is briefly summarized here. While standard MEP computations [15] are usually used for locating excited state paths from transition states on S_1, initial relaxation direction computations have been used here for locating excited state relaxation channels departing from non-stationary points such as FC. [16,17] This is accomplished first via locating an initial direction of relaxation (IRD) on S_1 (as close as possible to FC), [16,17] and second via standard minimum energy path computations following that IRD. Briefly, an IRD corresponds to a local *steepest descent direction,* in *mass-weighted cartesians,* from a given starting point. The IRD is calculated by

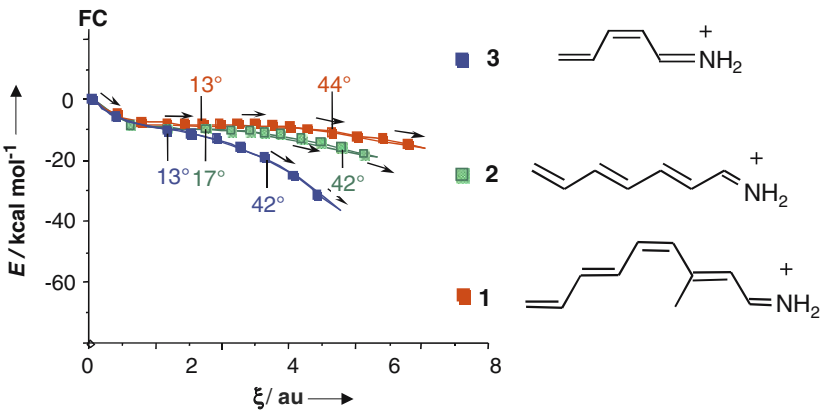

Scheme 1 CASPT2-scaled energy profiles along the reaction coordinate ξ[bohr (amu)$^{1/2}$] computed on S_1 for chromophore models (**1, 2** and **3**) of different chain lengths (bottom):[7–9] the twisting (in degrees) of the central double bond along the path is also reported

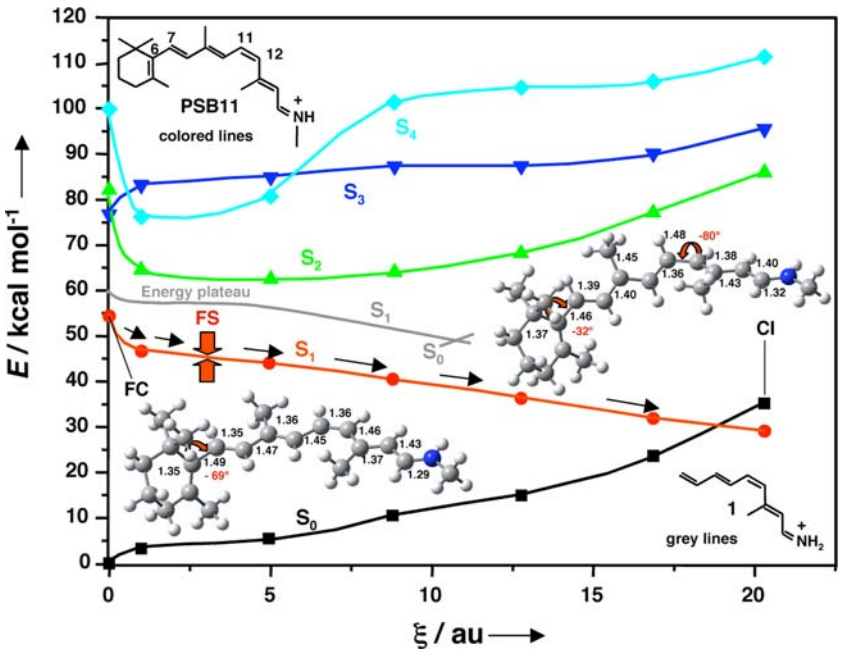

Fig. 1 CASPT2-scaled energy profiles along the CASSCF/6-31G* optimized reaction coordinate ξ [bohr (amu)$^{1/2}$] on S_1 (*black arrows*). Colors identify the electronic nature of the state. The FC and CI structures are also reported (in Å and degrees). *Gray lines* show the previously computed model **1** MEP [8]. The fluorescent state (FS) is assigned at 3 au (*red arrows*)

locating the energy minimum on a hyperspherical (i.e. $n-1$ dimensional) cross-section of the n dimensional potential energy surface (n is the number of vibrational degrees of freedom of the molecule) centered on the starting point (FC in this case). The radius of this hypersphere is usually chosen to be small (typically 0.25–0.5 au in *mass-weighted cartesians*) in order to locate the steepest direction in the vicinity of the starting point (i.e. the hypersphere center). The IRD is then defined as the vector joining the starting point to the energy minimum (an *hyperminimum*). Once the *hyperminimum* has been determined, the associated minimum energy path (emerging from these points) is computed as *the steepest descent line in mass-weighted cartesians* (au = bohr (amu)$^{1/2}$) using the IRD vector to define the initial direction to follow. These computations have been carried out with an home-made routine, plugged to the GAUSSIAN98 series of programs [18]. State-averaged CASPT2 computations [19] (equal weights have been used for S_0,S_1,S_2,S_3 and S_4) have been then performed on selected points along the S_1 MEP using the MOLCAS-6.0 package [20].

The MEP on the S_2 state has been built for a slightly different model of PSB11, where the methyl group (Me) of the protonated Schiff base has been replaced by a hydrogen atom, hereafter denoted as PSB11(R=H). That the spectroscopy of the full chromophore PSB11 (with R=Me so far employed) and PSB11(R=H) behave very similar has been very recently demonstrated [13]. The same holds true for the photochemical behavior along the S_1 MEP. For instance, for PSB11(R=H) the CI (S_0/S_1) structure is found with a similar twisting angle of the β-ionone ring (-39°) and rotation about the $C_{11}=C_{12}$ double bond (-80°) (cf. Fig. 1). Since the S_1 MEP for PSB11(R=H) leads to the same conclusion as analyzed below, it will not be discussed further. The S_2 MEP has been built as CASPT2//CASSCF/6-31G* steepest descendent paths in a procedure [21] (similar to the one described above) which is based on a modification of the projected constrained optimization (PCO) algorithm of Anglada and Bofill [22] and follows the Müller–Brown approach [23]. Each step requires the minimization (at the CASSCF level) of the potential energy surface (PES) on a hyperspherical cross section of the PES centered on the initial geometry and characterized by a predefined radius (0.3 au in this case). The optimized structure is taken as the center of a new hypersphere of the same radius, and the procedure is iterated until the bottom of the energy surface is reached. Mass-weighted coordinates [au = bohr (amu)$^{1/2}$] are used as well, such that the MEP coordinate corresponds to the so-called Intrinsic Reaction Coordinates (IRC). The full procedure is currently implemented in the MOLCAS-6.0 package [20] and its technical implementation has been published elsewhere [21]. At each optimized geometry, three singlet states were computed using the full active space of twelve active electrons in twelve orbitals (12e, 12o) and a state average procedure (equal weights have been used). Always, and in order to include the dynamic correlation effects, CASPT2 calculations were performed. At the final structure of the S_2 MEP, which is essentially coincident with the equilibrium geometry of the S_2 state, [13] an additional number of states have been computed.

It is worth mentioning that these relaxation channels (i.e. the MEPs) describe the *static* (i.e. *non-dynamical*) evolution of the system after photoexcitation and provide insight into the mechanism of molecular relaxation on S_1 and S_2 in conditions of vibrationally 'cold' molecules (i.e. with infinitesimal velocity). Although molecules have more than infinitesimal kinetic energy (and in fact classical trajectories deviate from this static path), nevertheless, minimum energy paths may represent a convenient measure of the progress of a molecule in a photochemical reaction, provided it occurs in a cold environment where slow excited state motion and/or thermal equilibration is possible (i.e. in a cold jet, or a cold matrix, or in solution) and the excited state reactant has a small/controlled amount of excess vibrational energy. Under these conditions, semiclassical dynamics yields the same mechanistic information as from topological investigation of the potential energy surface, because its structure is expected to play the dominant role in determining the molecular motion. This strategy has been successfully applied in previous computational investigations involving the photochemistry of neutral conjugated hydrocarbons [24–30] and PSBs [8,11,12,31–33] and has been validated by semiclassical dynamics computations [17,34,35]. While the analysis and discussion of these results are reported in the main text of the paper, the CASSCF and CASPT2 absolute energy values of all the relevant points are reported in the electronic supplementary material (see Table S1 and Table S2).

The efficiency (i.e. probability) of radiative transitions has been provided by the oscillator strength (*f*), which has been computed within the RASSI approach [36] using the CASPT2 corrected energies.

The charge distribution along the chromophore chain has been evaluated for the first five singlet states (S_0–S_4) described with state-averaged CASSCF wavefunctions by Mulliken-charges analysis and has been used to characterize the electronic nature (i.e. ionic vs. covalent) of the investigated states.

3 Results and discussion

3.1 Optical properties

The photoisomerization channel Figure 1 reports the behavior of the singlet manifold ($S_0 - S_4$), while Table 1 shows the evolution of the emission and transient absorption energies (and their oscillator strength *f*), along the computed MEP on S_1 (see the electronic supplementary material for absolute energy values), which describes the isomerization about the central $C_{11} = C_{12}$ bond of the chromophore.

Remarkably, the computed $S_0 \rightarrow S_1$ vertical transition energy for PSB11 (527 nm, i.e. 54.3 kcal mol^{-1}) agrees very well with the absorption value determined experimentally in Rh (500 nm, corresponding to ~57 kcal mol^{-1}) [2,14], while the absorption observed in solution (~450 nm) is recovered if a solvatochromic (blue) shift of ~9 kcal mol^{-1} is taken into account, as suggested by Gao et al. [37]. Emission and excited state transient absorptions may be tentatively assigned to the region along the reaction coordinate where the first impulsive motion (i.e. stretching) out of the Franck–Condon (FC) point has been completed, while the isomerization has not yet begun. This reasoning comes from a qualitative dynamical interpretation of the motion of the wavepacket along the MEP [7–9]. In fact, according to the *two-mode* reaction coordinate, internal vibrational energy redistribution must take place for the torsional (non totally symmetric) mode to get populated (i.e. vibrational energy must flow from the initially populated—totally symmetric—stretching motion to the torsional one) and this requires some time. Judiciously, this region (where the bonds have already relaxed but

Table 1 CASPT2-computed transitions (nm) and oscillator strengths (in brackets) along the computed S_1 MEP (in mass weighted coordinates au, see Fig. 1)

MEP (a.u)	S_0	S_1	S_2	S_3	S_4
0.00 (FC)	–	527 (0.858)	374 (0.020)	349 (0.268)	287 (0.026)
1.00	661 (1.243)	–	1612 (0.101)	971 (0.220)	785 (0.009)
3.00 (FS)	710	–	1700	930	740
5.00	744 (1.173)	–	1528 (0.148)	775 (0.284)	696 (0.061)
8.84	973 (0.646)	–	1205 (0.403)	609 (0.120)	469 (0.005)
12.77	1342 (0.467)	–	899 (0.519)	561 (0.200)	420 (0.009)
16.86	3473 (0.136)	–	634 (0.456)	492 (0.270)	387 (0.126)
20.31 (CI)	4697 (0.014)	–	504 (0.089)	431 (0.053)	349 (0.102)

While the values reported at the FC point correspond to absorptions from S_0, the other values refer to transitions from S_1 (i.e. emission and transient absorptions). Transition energies at the FS point have been estimated from the energy profiles in Fig. 1

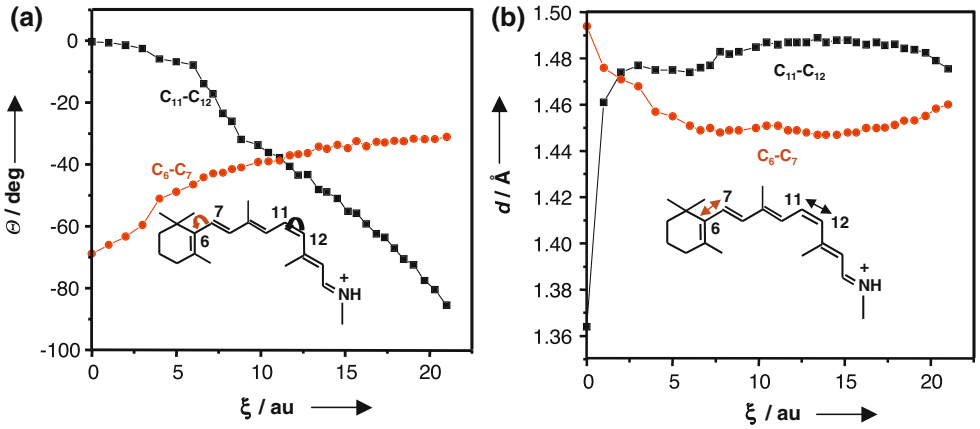

Fig. 2 Analysis of the S_1 reaction coordinate ξ [bohr (amu)$^{1/2}$] for the $C_{11} = C_{12}$ and the C_6–C_7 bonds: **a** twisting angles Θ and **b** bond lengths d

the torsions have not yet begun) is assigned as the fluorescent state (FS) since this is where the system will spend more time before it decays. Figure 2 provides an analysis of the reaction coordinate along the S_1 MEP, displaying the evolution of the $C_{11} = C_{12}$ and of the $C_6 - C_7$ twisting angles and bond lengths, respectively. This analysis reveals that the FS may be tentatively placed at about 3 au along the MEP (see red arrows in Fig. 1): here the central $C_{11} = C_{12}$ double bond has already fully elongated (from ∼1.36 to ∼1.48 Å) while its rotation has not yet started.

Remarkably, the estimated $S_1 \rightarrow S_0$ emission and $(S_4)S_3 \leftarrow S_1$ absorption around this point (see 1, 3 and 5 au in Table 1) are in reasonable agreement with the experimental data for the emission (∼650 nm) and near-IR excited state (transient) absorption (∼700 nm) in Rh [14] and well account for the competing stimulated emission and near-IR transient absorption observed [14], since it implies that in this region the S_1–$S_3(S_4)$ and S_1–S_0 energy gaps are similar.[1] The surprising agreement with the spectroscopic observations recorded in the protein leads to the remarkable and unintuitive suggestion that the isolated system is a good model for the optical properties of the chromophore in Rh, the effect of the protein environment being substantially *neutral* [38].

The gas phase and the protein: experiments and computations. A comparative analysis The aforementioned conclusion about the optical properties of the retinal chromophore and the claimed negligible effect of the protein environment deserve a deeper and thoughtful discussion in light of the very recent experimental observations recorded in the gas phase. Indeed, our statement seems to be in disagreement with the experimental absorption maximum of 610 nm which has been very recently recorded for the PSB11 chromophore in vacuo [39]. This value differs significantly from the absorption maximum observed in Rh (500 nm), apparently revealing that the effect of the protein environment is by no means globally neutral, as we claim. Besides, it is also significantly red-shifted from our computed value in the isolated PSB11 model (527 nm), questioning the quantitative validity of our model in vacuo. Anyway, a more careful analysis of the gas-phase data reveals a complex and structured absorption band with a secondary peak (or shoulder) around 530 nm. Note that this is a systematic feature of the spectra recorded in vacuo for all the different retinal PSB isomers investigated, and that this value is the one that we do predict by our computations (527 nm). It may be that this value corresponds to the energy for the pure vertical transition and that the complex feature of the band, as well as the 610 nm absorption maximum observed, is due to vibrational features. What we would like to emphasize here is that the aforementioned experimental result does not necessarily contradict our statement, since the recorded 610 nm absorption maximum could not be related to the pure vertical transition (which is in fact observed as a smaller peak at 530 nm) but, more simply, to a vibrational structure of the band.[2] Furthermore, this conclusion is in line with very recent computational results (including QM/MM computations on Rh) [38,40,41], which already suggest that the optical properties of the chromophore in Rh are about the same as computed in vacuo (note that this is not necessarily a property of all rhodopsin proteins). In agreement with that, our isolated retinal gives almost the same

[1] S_3 should be more easily populated (see the f values); prudently, S_4 has also been included here since both states are very close in energy around FS.

[2] A work on this topic is in preparation.

spectroscopic results as when included in Rh (527 vs. 500 nm absorption maximum, respectively), calling for a globally neutral effect of the protein.

Finally, also different hypothesis may be suggested, involving for example, the twisting of the β-ionone ring. Indeed, we have recently shown [13] that by twisting the ring a wide tuning in absorption energies for the retinal chromophore in vacuo may be achieved (Δ 140 nm, from 530 nm to 670 nm on going from the fully twisted to the planar ring, respectively). Thus, it is possible that in the experimental gas phase conditions, a slightly less twisted β-ionone ring (than the one predicted at this computational level) is responsible for the observed bathochromic shift. This would represent an alternative explanation to the aforementioned one based on the vibrational structure of the spectrum.

The complete elucidation of this issue would imply to carry out geometry optimization of the ground-state system at a correlated level, such as the MP2 method. Anyway, as far as our own experience is concerned, the MP2 geometries may be regarded as showing more conjugation than that obtained with CASSCF. MP2 tends to underemphasize the single–double bond alternation in PSBs and related compounds. This feature is connected with the previously well-documented effect that methodologies such as Møller–Plesset perturbation theory that are based on single reference wave functions, but that include large dynamic correlation corrections, usually overestimate π-conjugation [42]. On the other hand, CASSCF-optimized geometries have been successfully tested against experimental data for protonated Schiff bases by reproducing the vibrational structure of the resonance Raman (RR) spectra [33]. For this reason, it is believed that the CASSCF geometries are the closer to the actual gas-phase structure.

Furthermore, note that the vertical allowed S_0–S_1 transition recently computed with CASPT2 at the MP2 optimized geometry by Buss et al. [43] is red shifted by about 0.3 eV with respect to that obtained at the optimized CASSCF structure and, therefore, it is in apparent agreement with the band maximum (610 nm) recorded in the gas-phase absorption [39]. However, the S_0–S_2 vertical transition at the same level of theory is red shifted by 0.3 eV with respect to the corresponding observed band maximum [43]. Thus, the CASPT2 result obtained at the ground-state equilibrium MP2 geometry is able to match the S_0–S_1 observed gas-phase absorption maximum, but it does not work out so well for S_0–S_2.

At this point, we should keep in mind that the computed vertical transition does have not an experimental counterpart. In other words, there are no experimental *vertical transitions* to be compared with. One just has to recall, for instance, the spectroscopy of ethene itself, where there are clearly three different features: the 0–0, the band maximum, and the vertical transition, the latter of course estimated just on theoretical grounds. Thus, in order to perform a correct comparison to the observed band maximum, vibrational resolution of the band should be performed theoretically, a technically difficult task for a system of the molecular size of PSB11.[2] Alternatively, in the present case, the recorded band origin (T0) could correctly be compared to the computed value (strictly Te). The only difference between those two values is the zero point energy (ZPE) corrections, which are expected to cancel out to a large extent for the ground and excited state. For the trans-PSB conformer, the computed Te result for the lowest-energy band, 1.73 eV [13], is consistent within 0.1 eV with that observed by Nielsen et al. (see Fig. 2 in ref. [39]). This fact gives further support to the reliability of the optimized-CASSCF(12,12) structures, for both the ground and the lowest excited state.

In conclusion, it is worth mentioning that our 'vacuo = protein' statement is only qualitative and does refer to the spectroscopic properties of the chromophore only. It does not extend to mechanistic effects, e.g. quantum yields (QYs) and reaction rates. In fact, it is well known that its reactivity (e.g. the photoisomertization activity) does depend on the environment. For instance, photoisomerization QY in Rh (ca. 70%) is about four times greater than that in solution (ca. 15%), and the photoisomerization rate is more than seven times faster. Additionally, this does not apply to its structure, which is different in Rh as compared to that optimized in vacuo, as revealed by QM/MM computations by Sugihara et al. [44] and, previously, by Olivucci et al. [38]. For instance, the PSB11 chromophore in vacuo lacks the twists of the C11–C12 and the C12–C13 bonds, which are mainly due to interaction with the protein pocket and which may appear important in photoisomerization catalysis (see discussion in Sect. 3.3 below).

Unreactive population: the trap S_2 state Higher-lying singlet states have also been investigated as possible contributors to the spectroscopic properties. In particular, it is worth noting that the S_3 state placed vertically (FC structure) at 349 nm has a relatively high (0.3) *f* (see Table 1). Thus, to assess if this state can be populated (at least partially) by initial irradiation, the MEP on this state (hereafter called S_2 since it drops in energy and becomes S_2, see Fig. 1) has been computed (see Fig. 3).

As can be readily seen, pumping at 500 nm makes possible the population of both S_1 and S_2 (the S_0–S_2 (0–0) transition and the vertical emission from the S_2

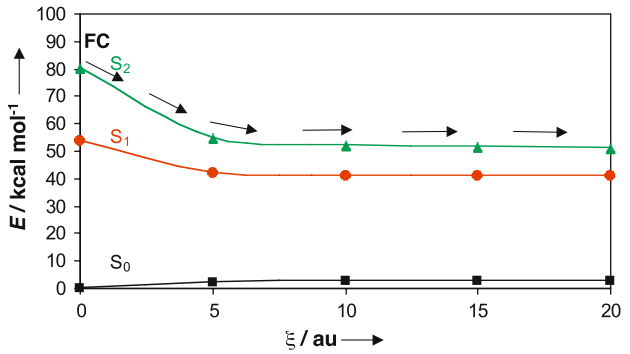

Fig. 3 CASPT2-scaled energy profiles along the optimized reaction coordinate ξ[bohr (amu)$^{1/2}$] on S_2 (*black arrows*)

minimum are computed to be 560 and 591 nm, respectively). That is, in principle, for a detailed discussion about the fluorescence of PSB11 both states have to be considered. Since S_2 is a bound state (i.e. it is unreactive, see Fig. 1) with a stable planar minimum, population on S_2 should live longer and may contribute to the emission.[3] It is worth noting that population of this state (a covalent – double H→L excitation—state, see Sect. 3.2 below) by a 500 nm irradiation wavelength should be much smaller compared to that of S_1 (although S_2 has a significant oscillator strength). Thus, the existence of a small unreactive population on S_2 is not in disagreement with the high photoisomerization QY observed.

Interestingly, the unreactive population recently detected in Rh [14] might be related to S_2, which would act as a *trap,* since it is well established by now that it does not participate in the photoisomerization. Although internal conversion of S_2–S_1 cannot be ruled out in principle (finally leading to the trans photoproduct), this process should occur in a much longer than the sub-picosecond timescale (see Ref. [9] where this problem is discussed) thus competing with radiative events. In this sense, it is worth mentioning that the observed 595–704 nm range of the excitation wavelength-dependent λ_{max} emission [45] points again to this state as being involved, since population of S_2 should depend on the excitation wavelength. Thus, the picture possibly resembles the emission of even polyenes like the paradigmatic *all-trans*-1,3,5,7-octatetraene, where both the 1^1B_u and 2^1A_g states do present fluorescence [46]. In particular, the new transient around 700 nm (~41 kcal mol^{-1}) present *before* and *after* the 580 nm photoproduct is formed (which is assigned to the non-isomerized population) [14], could be related to S_2. To assess this point, an additional number of states have been computed at the final structure of the S_2 MEP (i.e. the equilibrium geometry), see Table 2. In particular the $S_2 \rightarrow S_5$ transition computed at 737 nm (38.7 kcal mol^{-1}) is predicted with oscillator strength of 1.3 and appears as a good candidate for this transient absorption.

[3] A biexponential decay for the emission cannot be ruled out in this case, although IC to S1 may also occur, eventually leading to photoproduct formation in a slightly longer timescale.

Table 2 CASPT2 relative energies (ΔE in kcal mol^{-1}) and oscillator strengths (f) computed at the final point of the S_2 MEP

State	S_0	S_1	**S_2**	S_3	S_4	S_5
ΔE[a]	−48.4	−9.2	**0.00**[b]	25.8	30.0	38.7
f[c]	0.005	0.0003	–	0.030	0.116	1.273

[a] Imaginary level-shift 0.2 au
[b] The state is 51.1 kcal mol^{-1} above the S_0 minimum (FC structure)
[c] Referred to S_2

To summarize, a possible trapping-mechanism for the photoexcited population (involving the S_2 state) has been shown to be feasible, in agreement with recent experimental findings and providing an interpretation for these data. In particular, the S_2 state may contribute to both the fluorescence and transient absorption recorded in Rh, its importance and role depending most probably on the absorption wavelength. The elements supporting this novel view can be summarized here as follows:

(a) S_2 has not a negligible oscillator strength.
(b) Analysis of the S_2 surface (Fig. 3) reveals that it is not a reactive state (i.e. it is a trap state) and that it may be populated at 500 nm (although population must be much smaller compared to that of S_1, which is in agreement with the high photoisomerization QY and efficiency observed).
(c) The observed λ_{max} emission is excitation wavelength-dependent (from 595 to 704 nm) and this points again to this state as being involved, since population of S_2 should depend on the excitation wavelength.
(d) A transient absorption around 700 nm has been found from this state (see Table 2) that agrees with the experimentally detected one.

For these reasons, we think our statement is more than a simple suggestion: it is a founded hypothesis where, for the first time, all these evidences can be accounted for in a simple model. Obviously, this may not be the unique interpretation possible and, in fact, other explanations have been already presented in the past involving, for example, possible different forms of Rh, including unreactive species.

3.2 Charges analysis and electronic states characterization

Figure 4 reports the evolution of the chromophore Mulliken charges distribution along the computed MEP on S_1. Analysis of the charge distribution along the chromophore chain reveals that, as seen in previous works, the reactive excited state of PSB11 in vacuo is a hole-pair charge-transfer (i.e. a ionic) state along the whole MEP. That is, upon photoexcitation on S_1, the positive charge migrates from the Nitrogen-containing moiety towards the other half of the chromophore. Furthermore, its *ionic* character increases moving towards the CI, where the entire positive charge is located on the left moiety of the system. All the other states have a *covalent* (i.e. dot–dot) character and S_2,S_3 and S_4 do not mix with the S_1 spectroscopic state, i.e. they remain well-spaced (at least 17 kcal mol^{-1}) along the whole reactive process. That is, the photochemistry of this system is driven exclusively by an S_1 state with *ionic* nature (see also the supplementary material for further details).

3.3 Photoisomerization catalysis

The β-ionone ring effect Inspection of Fig. 2b reveals a concurrent (although less impulsive) shortening of the C_6–C_7 single bond along the S_1 MEP, the reason being its partial double bond character in S_1. This causes the simultaneous planarization of the β-ionone ring (see Fig. 2a), with its twisting angle passing from -69° in the FC point to -32° in the CI structure. This motion, which progressively turns the chromophore from a five to a six conjugated double bond system, may turn out to contribute to the efficient photoisomerization in the protein. In fact, according to the crystallographic structure (see Scheme 2) [47], Trp-265 is very close to the β-ionone ring (i.e. less than 3 Å) and, by twisting the C_6–C_7 bond (red arrow), the distance between the two groups dramatically shortens leading to steric interactions. Therefore, it is likely that in the protein the β-ionone ring acts like a *lever* upon planarization, forcing the central bond to twist *earlier* in the direction shown by the blue arrow: this increases the distance between the ring and Trp-265 and steric interactions

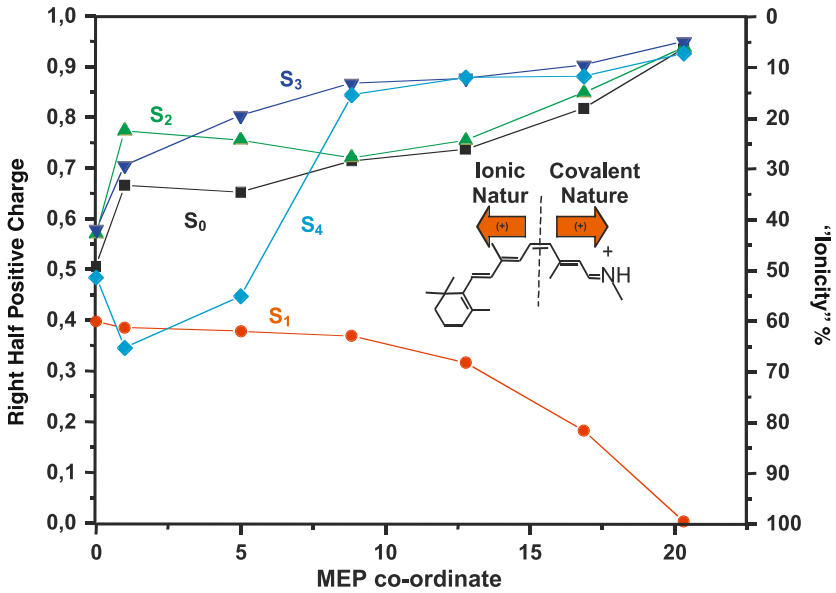

Fig. 4 Mulliken charges evolution along the MEP. The amount of charge in the right mojety (*dotted line* is the demarcation point) of the chromofore is reported, together with an indication of the "Ionicity character" of the wavefunction. S_1 is the only ionic state, S_0, S_2S_3 and S_4 show a covalent (i.e. dot–dot) character. The same convention as in Fig. 1 as been used here, with colors identifying each electronic state by its nature

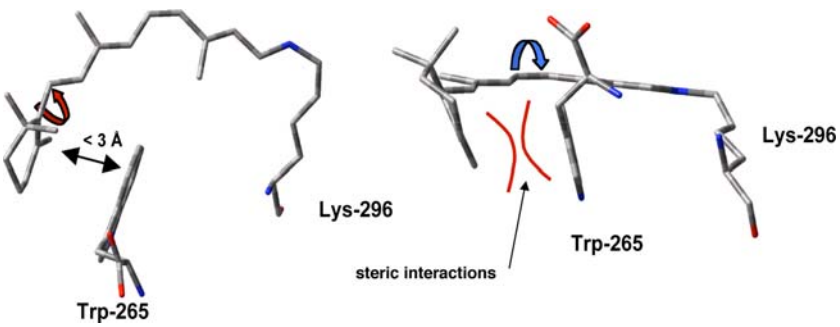

Scheme 2 Top (*left*) and a lateral (*right*) view of the chromophore binding pocket in Rh [50]

are reduced. Remarkably, this direction is in agreement with the sign of the initial $C_{11} = C_{12}$ twist which has been previously derived [38,44,48] in Rh. Together with the electrostatic catalysis and the intramolecular/intermolecular interactions discussed in previous works (see also below) [40,44,47,49,50], this provides a possible additional reason for the faster photoisomerization in the protein. That is, a *lever effect* would contribute in tilting the PES in such a way that the wavepacket would spend less time in the FS region and it would be more efficiently funneled into the rotational mode.

We may estimate quantitatively this effect by comparing the S_1 energy of the fully relaxed stationary point (SP) [13] with that of the relaxed chromophore taking the β-ionone ring frozen ($PSB11_{frozen}$), see Fig. 5. The contribution to the total relaxation energy due to the stretching process alone is $\sim 8\,kcal\,mol^{-1}$, while the one due *only* to the planarization of the ring is $\sim 7\,kcal\,mol^{-1}$, which may be addressed to the pure *lever effect* (see the electronic supplementary material for the CASPT2//CASSSCF/6-31g* absolute energy values). It is evident that this effect is far from being negligible and (although not alone) may improve the efficiency of the isomerization process in the protein compared to solution. We suggest this effect must be taken into account to properly understand protein catalysis, although it is not the only one operating in the protein: steric interactions on between the retinal C_{10}-Hydrogen and the C_{13} -methyl [50], electrostatic catalysis [40,41], twists about the $C_{11} = C_{12}$ and adjacent single bonds [44] and the close proximity of Cys-187 with the retinal C_{12} -Hydrogen [47,49] have proved to be involved in photoisomerization catalysis. Herein, we do not want to reject or question out these effects, but to highlight another possible cooperative mechanism, which is strictly related to an intrinsic property of the retinal chromophore (i.e. the excited state planarization of the β-ionone ring) and its subsequent interaction with the protein (namely Trp-265). This has never been revealed or discussed before. Whether this is a dominant, concurrent or secondary effect must be still estimated. Nevertheless, we have quantitatively evaluated such an effect showing here that it is not negligible (energetically) and thus it deserves consideration.

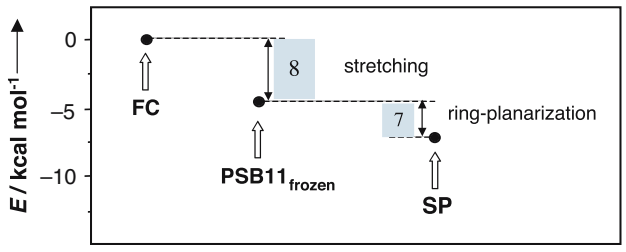

Fig. 5 CASPT2-corrected energy contributes to the initial relaxation energy on S_1 (SP data are from ref. [13])

It is worth noting that even IR difference spectra recently recorded [51] for a Rh with a modified acyclic retinal (i.e. lacking the β-ionone ring, thus preventing a level effect) do not help to evaluate this contribution. Although the Batho and Lumi intermediates are formed and Rh is activated (i.e. Meta II is formed), no information about the timescale and efficiency of the ultrafast primary event (i.e. the initial photoisomerization) is provided. Furthermore, Rh activation is not surprising since it primarily depends on the *cis* → *trans* isomerization of the central double bond of the chromophore, which in fact occurs also in other media (e.g. solution) in a longer (ps) timescale, in presence as well as in absence of the β-ionone ring (as experiments on modified retinals in solution show) [52–54].

Additionally, one may wonder how such a relay mechanism based on the lever effect could be achieved in the short time frame observed of about 100 fs. In fact, the lever (driven by the torque of the C_6–C_7 bond) would have to move the β-ionone ring and the complete ring system of Trp-265 against the central part of the chromophore, which involves up to 20 heavy atoms and it would also need an extremely fixed polyene backbone to transport the torque into the desired region. While this is a good reasoning (and in fact we say that the *lever effect* is only one of the possible contributors triggering the photoisomerization catalysis, see discussion above), it is a matter of fact that there is an intrinsic (7 kcal/mol energy driven) ability of the ring to get planar on S_1; as it is a matter of fact that this process leads to destabilization by steric interactions with Trp-265 in Rh (and that isomerization about the $C_{11} = C_{12}$ bond would relieve such a destabilization). Even a tiny motion in this direction may get rise to steric interactions with Trp-265. We do not necessarily need to wait for the full motion to take place and this effect could just provide an additional trigger for the ultrafast photoisomerization to occur. We believe we are fully consistent in saying that and what we have shown here is that there is a novel not negligible factor (due to the ring) that plays in favor of the $C_{11} = C_{12}$ bond isomerization. There is another point that directly comes from our computations: without such an effect (e.g. without the ring), the photoisomerization path would certainly be less favored, i.e. less steep or even with an energy barrier. Note in fact that the energy plateau seen in model 1 along the path (Fig. 1) does disappear in the real chromophore, which further supports this mechanism as one of the contributing effects for enhanced isomerization in Rh.

Finally, it is worth noting that single bond order increase is a general phenomenon for all single bonds in the excited state. In Rh (where also other single bonds such as C_{10}–C_{11} and C_{12}–C_{13} — are slightly twisted) [38,44,49] it can certainly play a role, contributing to photoisomerization catalysis. Anyway, the C_6–C_7 single bond is the most twisted one, both in vacuo as well as in Rh (i.e. it is almost fully deconjugated) [38,44,47,49]. Thus, here it is where this effect should be stronger. For these reasons we focused our attention onto this novel undocumented aspect, which is discussed here for the first time.

4 Conclusions

To summarize, we have provided computational evidences to the unintuitive view that PSB11 in isolated conditions is a good model for the spectroscopy of the chromophore in Rh. In addition, we have detected an accessible low lying state (S_2) which behaves as a trap (i.e. molecules pumped there do not isomerize) and which may be possibly involved in the formation of the unreactive population recently observed. Finally, by interaction with the surrounding residues (namely Trp-265), the β-ionone ring may origin (upon planarization) the spring effect necessary to trigger the efficient ultrafast isomerization seen in Rh (or at least it may contribute to that). In conclusion, these results suggest novel scenarios for the understanding of the spectroscopic observations recorded in Rh (including time resolved experiments) and the catalytic mechanism responsible for the highly efficient and ultrafast (i.e. sub-picosecond) photoisomerization. Furthermore, this work provides an accurate analysis of the intrinsic photoisomerization ability of the retinal chromophore and constitutes a solid reference for further studies aimed to rationalize the effect of the environment on its photochemical behavior.

Acknowledgment Funds for Selected Research Topics, MURST PRIN 2005 (project: "Trasferimenti di energia e di carica a livello molecolare"), FIRB (RBAU01L2HT) and Spanish MEC-FEDER CTQ2004-01739 are gratefully acknowledged.

References

1. Kandori H, Shichida Y, Yoshizawa T (2001) Biochemistry-Moscow 66:1197–1209
2. Needleman R (1995) In: Horspool WM, Song P-S (Eds) CRC handbook of organic photochemistry and photobiology. CRC Press, Boca Raton, pp. 1508–1515
3. Ottolenghi M, Sheves M (1995) Is J Chem 35:U3–U3
4. Wald G (1968) Science 162:230–239
5. Mathies R, Lugtenburg J (2000) In: Stavenga DG, DeGrip WJ, Pugh ENJ (Eds) Molecular mechanism of vision. Elsevier Science Press, New York, pp. 55–90
6. Yoshizawa T, Kuwata O (1995) In: Horspool WM, Song P-S (Eds) CRC handbook of organic photochemistry and photobiology. Boca Raton, FL pp. 1493–1499
7. Garavelli M, Bernardi F, Olivucci M, Vreven T, Klein S, Celani P, Robb MA (1998) Faraday Discuss 110:51–70
8. González-Luque R, Garavelli M, Bernardi F, Merchán M, Robb MA, Olivucci M (2000) Proc Natl Acad Sci USA 97:9379–9384
9. Cembran A, Bernardi F, Olivucci M, Garavelli M (2003) J Am Chem Soc 125:12509
10. De Vico L, Page CS, Garavelli M, Bernardi F, Basosi R, Olivucci M (2002) J Am Chem Soc 124:4124–4134
11. Garavelli M, Vreven T, Celani P, Bernardi F, Robb MA, Olivucci M (1998) J Am Chem Soc 120:1285–1288
12. Garavelli M, Celani P, Bernardi F, Robb MA, Olivucci M (1997) J Am Chem Soc 119:6891–6901
13. Cembran A, González-Luque R, Altoè P, Merchán M, Bernardi F, Olivucci M, Garavelli M (2005) J Phys Chem A 109:6597–6605
14. Haran G, Morlino EA, Matthes J, Callender RH, Hochstrasser RM (1999) J Phys Chem A 103:2202–2207
15. Bearpark MJ, Robb MA, Schlegel HB (1994) Chem Phys Lett 223:269–274
16. Celani P, Robb MA, Garavelli M, Bernardi F, Olivucci M (1995) Chem Phys Lett 243:1–8
17. Garavelli M, Celani P, Fato M, Bearpark MJ, Smith BR, Olivucci M, Robb MA (1997) J Phys Chem A 101:2023–2032
18. Gaussian 98 (1998) Gaussian Inc., Pittsburgh PA
19. Andersson K, Malmqvist PA, Roos BO (1992) J Chem Phys 96:1218–1226
20. MOLCAS (2004) Department of Theoretical Chemistry, Chemical Centre, University of Lund, Lund
21. De Vico L, Olivucci M, Lindh R (2005) J Chem Theory Comp 1:1029
22. Anglada JM, Bofill JM (1997) J Comput Chem 18:992
23. Müller K, Brown LD (1979) Theor Chim Acta 53:75
24. Garavelli M, Bernardi F, Cembran A, Castano O, Frutos LM, Merchán M, Olivucci M (2002) J Am Chem Soc 124:13770–13789
25. Garavelli M, Bernardi F, Moliner V, Olivucci M (2001) Angew Chem Int Ed Engl 40:1466
26. Garavelli M, Celani P, Bernardi F, Robb MA, Olivucci M (1997) J Am Chem Soc 119:11487–11494
27. Fuss W, Haas Y, Zilberg S (2000) Chem Phys 259:273–295
28. Garavelli M, Frabboni B, Fato M, Celani P, Bernardi F, Robb MA, Olivucci M (1999) J Am Chem Soc 121:1537–1545
29. Garavelli M, Page CS, Celani P, Olivucci M, Schmid WE, Trushin SA, Fuss W (2001) J Phys Chem A 105:4458–4469
30. Garavelli M, Smith BR, Bearpark MJ, Bernardi F, Olivucci M, Robb MA (2000) J Am Chem Soc 122:5568–5581
31. Garavelli M, Bernardi F, Celani P, Robb MA, Olivucci M (1998) J Photochem Photobiol A 114:109–116
32. Garavelli M, Bernardi F, Robb MA, Olivucci M (1999) J Mol Struct 463:59–64
33. Garavelli M, Negri F, Olivucci M, (1999) J Am Chem Soc 121:1023–1029
34. Vreven T, Bernardi F, Garavelli M, Olivucci M, Robb MA, Schlegel HB (1997) J Am Chem Soc 119:12687–12688
35. Garavelli M, Bernardi F, Olivucci M, Bearpark MJ, Klein S, Robb MA (2001) J Phys Chem A 105:11496–11504
36. Malmqvist P-Å, Roos BO (1989) Chem Phys Lett 155:189
37. Rajamani R, Gao J (2002) J Comput Chem 23:96–105

38. Andruniów T, Ferré N, Olivucci M (2004) Proc Natl Acad Sci USA 101:17908–17913
39. Nielsen IB, Lammich L, Andersen LH (2006) Phys Rev Lett 96:018304–018301, 018304–018304
40. Cembran A, Bernardi F, Olivucci M, Garavelli M (2004) J Am Chem Soc 126:16018–16037
41. Cembran A, Bernardi F, Olivucci M, Garavelli M (2005) Proc Natl Acad Sci USA 102:6255–6260
42. Bifone A, de Groot HJM, Buda F (1996) Chem Phys Lett 248:165–172
43. Sekharan S, Weingart O, Buss V (2006) Biophys J 91:L07–L09
44. Sugihara M, Hufen J, Buss V (2006) Biochemistry 45:801–810
45. Kochendoerfer GG, Mathies RA (1996) J Phys Chem 100
46. Serrano-Andrés L, Lindh R, Roos BO, Merchán M (1993) J Phys Chem 97:9360
47. Teller DC, Okada T, Behnke CA, Palczewski K, Stenkamp RE (2001) Biochemistry 40:7761–7772
48. Buss V, Kolster K, Terstegen F, Vahrenhorst R (1998) Angew Chem Int Ed Engl 37:1893–1895
49. Okada T, Sugihara M, Bondar AN, Elstner M, Buss V (2004) J Mol Biol 342:571–583
50. Kochendoerfer GG, Verdegem PJE, vanderHoef I, Lugtenburg J, Mathies RA (1996) Biochemistry 35:16230–16240
51. Bartl FJ, Fritze O, Ritter E, Herrmann R, Kuksa V, Palczewski K, Hofmann KP, Ernst OP (2005) J Mol Biol 280:34259–34267
52. Albeck A, Livnah N, Gottlieb H, Sheves M (1992) J Am Chem Soc 114:2400–2411
53. Arnaboldi M, Motto MG, Tsujimoto K, Balogh-Nair V, Nakanishi K (1979) J Am Chem Soc 101:7082–7084
54. Bologh-Nair V, Carriker JD, Honig B, Kamat V, Motto MG, Nakanishi K, Sen R, Sheves M, Arnaboldi M, Tsujimoto K (1981) Photochem Photobiol 33:483–488